

Original Article

Susceptibility weighted angiography in demonstration of veins and arteries of cerebral gliomas

Wenfeng Xiao^{1,2}, Qing Zhang³, Ying Huang², Chuanting Li¹, Chuanmei Liu¹, Guodong Wang⁴, Lebin Wu¹

¹Shandong Medical Imaging Research Institute, Shandong University, Jinan 250021, China; ²Shengli Oilfield Central Hospital, Dongying 257034, China; ³Jinan Central Hospital, Shandong University, Jinan 250021, China; ⁴Shandong Provincial Hospital, Shandong University, Jinan 250021, China

Received November 14, 2015; Accepted March 26, 2016; Epub May 15, 2016; Published May 30, 2016

Abstract: Background: This study aimed to assess the potential of susceptibility weighted angiography (SWAN) in the demonstration of both veins and arteries in cerebral gliomas, and evaluate its value in grading these tumors. Methods: 26 patients with cerebral gliomas (grade I-II: n = 11; grade III-IV: n = 15) received conventional imaging examination and 3D multi-echo gradient echo T2 star weighted angiography. Both MinIP and MaxIP images were reconstructed to depict both veins and arteries in the gliomas. The veins and arteries in SWAN images were analyzed and compared. Results: The arteries were depicted in SWAN MaxIP images, and the veins in SWAN MinIP images. The arteries could be distinguished from the veins. The amount of veins and arteries in SWAN images was correlated strongly with pathology. The veins and arteries of cerebral gliomas in SWAN images differed significantly. Conclusion: SWAN allows for high-resolution visualization of both veins and arteries of the cerebral gliomas in one sequence without application of contrast agent by using of MinIP and MaxIP reconstructions, which plays an important role in grading of these tumors.

Keywords: Susceptibility weighted angiography, cerebral glioma, magnetic resonance imaging

Introduction

Susceptibility weighted imaging (SWI) takes advantage of the “magnetic susceptibility”, which is defined as the magnetic response of a substance when it is placed in an external magnetic field. In magnetic resonance imaging (MRI), it is well known that venous blood due to its high amount of deoxygenated hemoglobin has paramagnetic properties and therefore also a high susceptibility. SWI is widely used to evaluate the hemorrhagic foci, iron deposition, and small venous vasculature of the brain [1-3]. Calculating weighted sum of the images obtained at different echo times results in heavy susceptibility weighted images. It is possible to combine the information of these multiple echo susceptibility weighted images with a first echo using the arterial inflow (time of flight, TOF) effect to simultaneously visualize both cerebral veins and arteries. This combined approach was used in our study with a three dimensional (3D) multi-echo gradient echo

sequence, also known as susceptibility weighted angiography (SWAN) [4-6]. Vascular growth in tumors plays an important role in the grading of cerebral gliomas. The amount of small veins in astrocytomas has been shown to correlate with tumor grade [7, 8]. This study was to assess the potential of SWAN for the depiction of both veins and arteries in the cerebral gliomas, and to evaluate its value in grading these tumors.

Material and methods

Patients

This study has been approved by the Ethics Committee of Shandong Medical Imaging Research Institute (2015-14-2S). A total of 26 cerebral glioma patients (males: n = 14; females: n = 12) with the median age of 49.1 years (range: 17-79 years) were recruited into present study. All the patients signed informed consent, and the Institutional Review Board of our hospital approved this study. There were 16 patients

Susceptibility weighted angiography in cerebral glioma

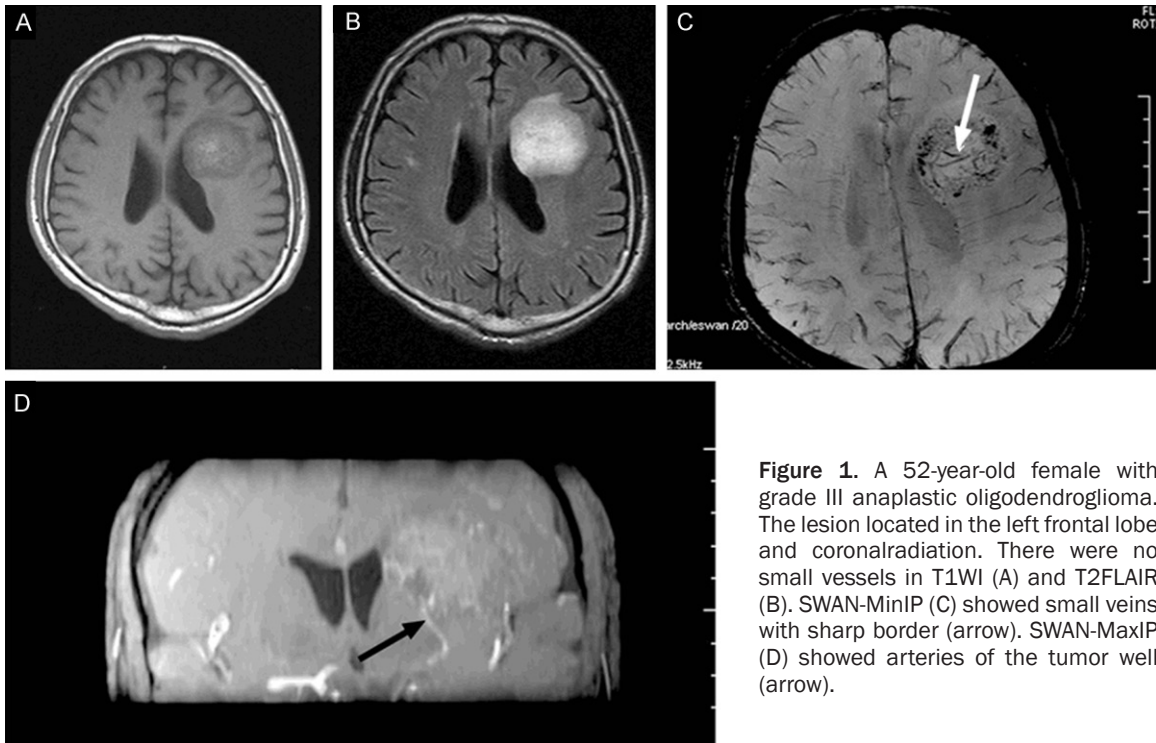


Figure 1. A 52-year-old female with grade III anaplastic oligodendroglioma. The lesion located in the left frontal lobe and coronalradiation. There were no small vessels in T1WI (A) and T2FLAIR (B). SWAN-MinIP (C) showed small veins with sharp border (arrow). SWAN-MaxIP (D) showed arteries of the tumor well (arrow).

who complained of dizziness and headache for 5 days to 2 years; 6 had limb asthenia; 4 developed nausea and vomiting; 1 had hemi-anesthesia. Cerebral gliomas were classified according to the 2007 World Health Organization (WHO) classification system for the central nervous system tumors [9]. Patients were divided into 2 groups according to the grade of cerebral gliomas: grade I-II (low grade) group and grade III-IV (high grade) group. Of 11 patients in low-grade group, 2 were diagnosed with grade II diffuse fibrillary glioma, 4 with a grade I or grade II pilocytic astrocytoma, 3 with grade II oligodendroglioma, and 2 with grade II oligoastrocytoma. Of 15 patients in high grade group, 5 were diagnosed with grade IV glioblastoma multiforme, 6 with grade III anaplastic astrocytoma, and 4 with grade III anaplastic oligodendroglioma. Patients in both groups didn't receive radiotherapy and chemotherapy before MR examination, and diagnosis was pathologically proven. The findings shown in the MR sequences were compared with those in pathology.

MR imaging protocol

MRI was performed on a 3.0 T MR scanner (Signa HDxt GE Healthcare) using an 8 channel head coil. Conventional imaging techniques

(T1WI, T2WI, T2FLAIR and CE-T1WI) and 3D multi-echo gradient echo T2 star weighted angiography sequence were used. The parameters of conventional MR sequences used were as follows: T1-Weighted spin echo fluid attenuated inversion recovery (FLAIR) images (TR: 2580 ms, TE: 23 ms, TI: 860 ms), T2-Weighted fast spin echo images (TR: 4600 ms, TE: 110 ms), T2-Weighted FLAIR images (TR: 9602 ms, TE: 117 ms, TI: 2400 ms), and enhanced T1 Weighted spin echo FLAIR images. Slice thickness and slice interval was 5.0\1.5 mm. FOV was 240 mm×240 mm. Gadolinium chelate as a contrast was injected at 0.1 mmol/kg.

The parameters of SWAN were as follows: TR = 43 ms, TE = 4.4-49 ms with 8 echoes, slice thickness = 2 mm, flip angle = 15°, bandwidth = 62.5 Hz, FOV = 240 mm×240 mm, matrix = 256×224. Both minimum intensity projections (MinIP) and maximum intensity projections (MaxIP) images were reconstructed to depict both veins and arteries of the cerebral gliomas. The veins and arteries both within and at the margins of cerebral gliomas in SWAN images were analyzed, and the total veins and arteries within the tumors were counted. The differences in SWAN images were compared between two groups.

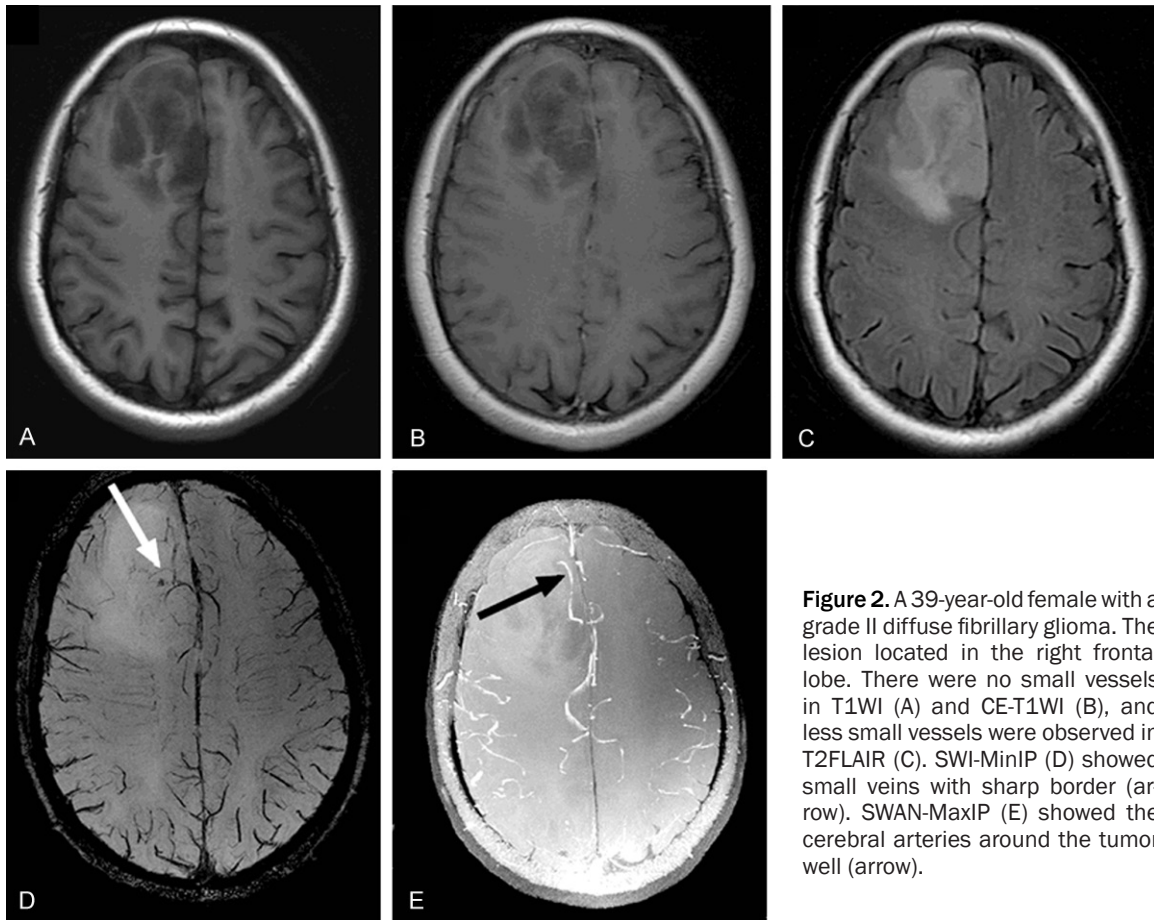


Figure 2. A 39-year-old female with a grade II diffuse fibrillary glioma. The lesion located in the right frontal lobe. There were no small vessels in T1WI (A) and CE-T1WI (B), and less small vessels were observed in T2FLAIR (C). SWI-MinIP (D) showed small veins with sharp border (arrow). SWAN-MaxIP (E) showed the cerebral arteries around the tumor well (arrow).

Data post-processing and analysis

Data post-processing was performed interactively using the multiplanar reconstruction of a standard workstation (AW workstation, GE Healthcare, Milwaukee, USA). MinIP and MaxIP of the SWAN sequence (SWAN-MinIP, and SWAN-MaxIP, respectively) were obtained. The images were reviewed independently by two experienced radiologists (L.C and W.L) who evaluated the quality of vessel identification using the 4-point scoring system: 0: not identified; 1: identified, but not continuously; 2: identified continuously, but with a heterogeneous signal; 3: identified continuously, and with a homogeneous signal.

Statistical analysis

Statistical analysis was performed with SPSSIBM (Armonk, NY). The scores of cerebral arteries and veins in opposite hemisphere of tumors between two experienced neuroradiologists were compared by using non-parametric

two-sample Wilcoxon test. The generalized kappa (κ) of Fleiss was used as a measurement of agreement among two blinded evaluators. Wilcoxon test for two independent samples was used to analyze the differences between two groups in terms of the tumor arteries and veins displayed on the SWAN sequence. A value of $P < 0.05$ was considered statistically significant.

Results

The quality of cerebral arteries and veins in opposite hemisphere of tumors in SWAN images

The cerebral arteries in opposite hemisphere of gliomas were depicted in SWAN MaxIP images, and the veins in SWAN MinIP images (**Figures 1, 2**). Two neuroradiologists evaluated the quality of cerebral arteries and veins in opposite hemisphere of gliomas in SWAN images using the 4-point scoring system. Results are shown in **Table 1**. In 26 cerebral glioma patients, cerebral arteries and veins in opposite hemisphere

Susceptibility weighted angiography in cerebral glioma

Table 1. Scores in terms of quality of arteries and veins in opposite hemisphere of tumors in SWAN images ($\bar{x} \pm s$)

| Item | Valuator 1 | Valuator 2 | Kappa | P |
|---|------------|------------|-------|-------|
| Cerebral arteries in opposite hemisphere of tumors (n = 26) | 1.82±0.61 | 1.94±0.51 | 0.82 | >0.05 |
| Cerebral veins in opposite hemisphere of tumors (n = 26) | 2.31±0.42 | 2.19±0.35 | 0.89 | >0.05 |

Table 2. The tumor arteries and veins in SWAN images in different grades of cerebral gliomas ($\bar{x} \pm s$)

| Item | High grade (n = 15) | Low grade (n = 11) | P |
|--------------------------|------------------------|-----------------------|--------|
| Amount of tumor veins | 18.42±11.91 | 9.89±8.12 | <0.001 |
| Amount of tumor arteries | 8.84±4.51 | 3.19±3.05 | <0.001 |

of gliomas in SWAN images could be identified as about score 2 (identified continuously, but with a heterogeneous signal). The identification of veins in opposite hemisphere of gliomas was better than that of arteries although there was no significant difference ($P > 0.05$). The identification score of cerebral arteries and veins in opposite hemisphere of tumors between two neuroradiologists was consistent, and there was no significant difference. The visualization of both cerebral veins and arteries could be displayed in SWAN sequence with high quality.

The arteries and veins of SWAN images in different grades of cerebral gliomas

The arteries of cerebral gliomas were depicted in SWAN MaxIP images, and the veins in SWAN MinIP images (**Figures 1, 2**). The tumor arteries and veins of SWAN images in different grades of cerebral gliomas are shown in **Table 2**. The amount of veins and arteries in SWAN images of cerebral gliomas were correlated strongly with pathological findings. The amount of veins and arteries in SWAN images was significantly different among different grades of cerebral gliomas ($P < 0.001$). The amount of both tumor veins and arteries in high grade gliomas were more than that in low grade gliomas.

Discussion

Deoxyhaemoglobin in the venous blood acts as an intrinsic contrast agent, causing $T2^*$ related loss in magnitude and a shift relative to the surrounding tissues in the phase images. The iron in oxyhaemoglobin is shielded by oxygen, and thus the $T2^*$ and susceptibility effects are only observed in venous blood. This provides a natural signal contrast between venous and arterial

blood. Hence, MRI with a long TE tends to distinguish arteries from veins. Apart from the $T2^*$ shortening, the bulk susceptibility shift effect of the deoxygenated blood causes a frequency shift of the protons, which leads ultimately to a phase difference between venous blood spins and tissue spins.

Veins are dark because of $T2^*$ loss, whereas arteries are bright because of TOF in the flow enhancement [4, 10, 11]. Selecting the proper TE is particularly important in application of the single-echo approach. In fact, TE selection is a compromise because a long TE increases the venous contrast but results in flow-related loss in rapidly flowing arteries, whereas a short TE has a lower degree of SWI [12].

SWAN is a 3D multi-echo gradient-echo pulse sequence with partial flow compensation. SWAN uses only magnitude, not phase information, of MR signals from tissues and theoretically offers a different tissue contrast from 3D susceptibility weighted imaging, which utilizes both magnitude and phase information. The SWAN-sequence uses multiple magnitude images with different echo times for the image generation [13, 14]. In our study, multiple phase and magnitude images at 8 echo times were acquired within a single scan. In this way, the sensitivity of the SWAN sequence to susceptibility effects was enhanced at longer echo times. This technique avoids complex post-processing as compared to other SWI approaches. The averaging of several images also leads to a higher signal to noise ratio in resulting susceptibility weighted images. As the several echoes are collected within one TR, the acquisition time is not prolonged as compared to the duration needed to acquire a single echo [15]. A disadvantage of the SWAN approach might be the loss of information due to the fact that phase information is not taken into account.

Our findings indicated that SWAN allows the identification and differentiation of cerebral and tumor veins and arteries in one sequence without the administration of intravenous con-

trast agent. By use of either MinIP or MaxIP reconstruction, arteries may be distinguished from veins [13, 16]. The anatomical details of the vasculature were identified continuously, but with a heterogeneous signal. The scan time of SWAN was significantly shorter than the combined scan time of artTOF and venTOF. The clinical relevance of SWAN as compared to the existing non-contrast MRA technique as gold standard should be further evaluated in systematic studies [17, 18]. The results of Chen's study has shown that SWAN scan time is significantly faster compared with the sum of both 3D-TOF MRA and 2D-TOF MR Venography, which results in significantly decreased patient discomfort and specific absorption rate. The use of simultaneous acquisition of MRA and MRV could eliminate the possible misregistration between the arterial and venous vasculatures, which could be induced by patient motion during acquisition, and it would greatly benefit clinicians to distinguish the exact spatial relationship between the arterial and venous vasculatures at or near the lesions [19]. By imaging both arteries and veins, more complete images of the vasculature of the brain and gliomas were created in our study. The advantage of collecting both arteries and veins of the gliomas in a single acquisition is that there will be no registration artifacts and that their relationship with each other with the gliomas and adjacent brain structure can be carefully reviewed.

The accurate grading of brain lesions has important prognostic and therapeutic implications, because high-grade lesions are treated differently from low-grade lesions. Patients with high grade lesions resectable or unresectable usually receive either radiotherapy or radiochemotherapy. Low grade gliomas are often treated by surgical resection with curative intent, and adjuvant radiochemotherapy is only recommended for grade II glioma patients with complete resection or those older than 40 years regardless of the extent of resection. Various image characteristics have been suggested to be predictors of glioma grade in humans, including heterogeneity, contrast enhancement, mass effect, cyst formation or necrosis, metabolic activity and cerebral blood volume. Susceptibility weighted imaging is better to define the internal architecture of the brain tumor as compared to conventional MR sequence [20-22]. In our study, SWAN images

depicted arterial blood supply and venous drainage of the cerebral gliomas in the same sequence, which is helpful for the surgical treatment. SWAN sequence displayed the average number of veins was 18.42 and that of arteries was 8.84 in high-grade cerebral gliomas, and, in low grade gliomas, the average number of veins was 9.89 and that of arteries was 3.19, showing significant difference between two groups at different grades of cerebral gliomas. The amount of vasculature is correlated with extent of angiogenesis in the cerebral gliomas. This technique may be promising for the non-invasive differentiation of low grade cerebral gliomas from high grade cerebral gliomas.

Conclusions

In conclusion, SWAN allows for high resolution visualization of both veins and arteries of the cerebral gliomas in one sequence by using of MinIP and MaxIP reconstructions, which plays an important role in grading of these tumors.

Disclosure of conflict of interest

None.

Address correspondence to: Chuanting Li, Shandong Medical Imaging Research Institute, Shandong University, Jinan 250021, China. E-mail: lichuanting-doc@163.com

References

- [1] Thomas B, Somasundaram S, Thamburaj K, Kesavadas C, Gupta AK, Bodhey NK and Kapilamoorthy TR. Clinical applications of susceptibility weighted MR imaging of the brain-a pictorial review. *Neuroradiology* 2008; 50: 105-116.
- [2] Mittal S, Wu Z, Neelavalli J and Haacke EM. Susceptibility-weighted imaging: technical aspects and clinical applications, part 2. *AJNR Am J Neuroradiol* 2009; 30: 232-252.
- [3] Haacke EM, Mittal S, Wu Z, Neelavalli J and Cheng YC. Susceptibility-weighted imaging: technical aspects and clinical applications, part 1. *AJNR Am J Neuroradiol* 2009; 30: 19-30.
- [4] Reichenbach JR, Venkatesan R, Schillinger DJ, Kido DK and Haacke EM. Small vessels in the human brain: MR venography with deoxyhemoglobin as an intrinsic contrast agent. *Radiology* 1997; 204: 272-277.

Susceptibility weighted angiography in cerebral glioma

- [5] de Souza JM, Domingues RC, Cruz LC Jr, Domingues FS, Iasbeck T and Gasparetto EL. Susceptibility-weighted imaging for the evaluation of patients with familial cerebral cavernous malformations: a comparison with t2-weighted fast spin-echo and gradient-echo sequences. *AJNR Am J Neuroradiol* 2008; 29: 154-158.
- [6] Hodel J, Blanc R, Rodallec M, Guillonnet A, Gerber S, Pistocchi S, Sitta R, Rabrait C, Zuber M, Pruvo JP, Zins M and Leclerc X. Susceptibility-weighted angiography for the detection of high-flow intracranial vascular lesions: preliminary study. *Eur Radiol* 2013; 23: 1122-1130.
- [7] Li C, Ai B, Li Y, Qi H and Wu L. Susceptibility-weighted imaging in grading brain astrocytomas. *Eur J Radiol* 2010; 75: e81-85.
- [8] Zhang H, Tan Y, Wang XC, Qing JB, Wang L, Wu XF, Zhang L and Liu QW. Susceptibility-weighted imaging: the value in cerebral astrocytomas grading. *Neurol India* 2013; 61: 389-395.
- [9] Louis DN, Ohgaki H, Wiestler OD, Cavenee WK, Burger PC, Jouvet A, Scheithauer BW and Kleihues P. The 2007 WHO classification of tumours of the central nervous system. *Acta Neuropathol* 2007; 114: 97-109.
- [10] Reichenbach JR, Jonetz-Mentzel L, Fitzek C, Haacke EM, Kido DK, Lee BC and Kaiser WA. High-resolution blood oxygen-level dependent MR venography (HRBV): a new technique. *Neuroradiology* 2001; 43: 364-369.
- [11] Du YP, Jin Z, Hu Y and Tanabe J. Multi-echo acquisition of MR angiography and venography of the brain at 3 Tesla. *J Magn Reson Imaging* 2009; 30: 449-454.
- [12] Barnes SR and Haacke EM. Susceptibility-weighted imaging: clinical angiographic applications. *Magn Reson Imaging Clin N Am* 2009; 17: 47-61.
- [13] Boeckh-Behrens T, Lutz J, Lummel N, Burke M, Wesemann T, Schopf V, Bruckmann H and Linn J. Susceptibility-weighted angiography (SWAN) of cerebral veins and arteries compared to TOF-MRA. *Eur J Radiol* 2012; 81: 1238-1245.
- [14] Hodel J, Leclerc X, Khaled W, Tamazyan R, Rodallec M, Gerber S, Blanc R, Benadjaoud M, Lambert O, Rabrait C, Zuber M, Rahmouni A and Zins M. Comparison of 3D multi-echo gradient-echo and 2D T2* MR sequences for the detection of arterial thrombus in patients with acute stroke. *Eur Radiol* 2014; 24: 762-769.
- [15] Hayashida Y, Kakeda S, Hiai Y, Ide S, Ogasawara A, Ooki H, Watanabe K, Nishimura J, Ohnari N and Korogi Y. Diagnosis of intracranial hemorrhagic lesions: comparison between 3D-SWAN (3D T2*-weighted imaging with multi-echo acquisition) and 2D-T2*-weighted imaging. *Acta Radiol* 2014; 55: 201-207.
- [16] Gang Q, Zhang J, Hao P and Xu Y. Detection of hypoxic-ischemic brain injury with 3D-enhanced T2* weighted angiography (ESWAN) imaging. *Eur J Radiol* 2013; 82: 1973-1980.
- [17] Hodel J, Rodallec M, Gerber S, Blanc R, Maraval A, Caron S, Tyvaert L, Zuber M and Zins M. [Susceptibility weighted magnetic resonance sequences "SWAN, SWI and VenobOLD": technical aspects and clinical applications]. *J Neuroradiol* 2012; 39: 71-86.
- [18] Kunimatsu A, Suzuki Y, Hagiwara K, Sasaki H, Mori H, Katsura M and Ohtomo K. Clinical value of 3D T(2)*-weighted imaging with multi-echo acquisition: comparison with conventional 2D T(2)*-weighted imaging and 3D phase-sensitive MR imaging. *Magn Reson Med Sci* 2012; 11: 205-211.
- [19] Chen L, Zhang J, Wang QX, Peng L, Luo X, Zhu WZ, Roshan AK, Qi JP and Wang H. Enhanced susceptibility-weighted angiography (ESWAN) of cerebral arteries and veins at 1.5 Tesla. *Br J Radiol* 2014; 87: 20130486.
- [20] Wang XC, Zhang H, Tan Y, Qin JB, Wu XF, Wang L and Zhang L. Combined value of susceptibility-weighted and perfusion-weighted imaging in assessing who grade for brain astrocytomas. *J Magn Reson Imaging* 2014; 39: 1569-1574.
- [21] Ding Y, Xing Z, Liu B, Lin X and Cao D. Differentiation of primary central nervous system lymphoma from high-grade glioma and brain metastases using susceptibility-weighted imaging. *Brain Behav* 2014; 4: 841-849.
- [22] Di Ieva A, God S, Grabner G, Grizzi F, Sherif C, Matula C, Tschabitscher M and Trattinig S. Three-dimensional susceptibility-weighted imaging at 7 T using fractal-based quantitative analysis to grade gliomas. *Neuroradiology* 2013; 55: 35-40.